Distributed Online Monitoring of Quasi-Static Voltage Collapse in Multi-Area Power Systems

Le Xie, *Member, IEEE*, Yang Chen, *Student Member, IEEE*, and Huaiwei Liao, *Member, IEEE*

***Abstract*—This paper presents a novel performance index for distributed monitoring of quasi-static voltage collapse in multi-area interconnected power systems. Based on the sensitivity of the smallest singular value of the power flow Jacobian matrix with respect to the regional load vector, the performance index applies *overlapping decomposition* in order to monitor the entire interconnected system with minimal area-level information exchange. Theoretical justification and practical implementation of distributed voltage stability monitoring are presented. By comparing the value of the performance index with a numerically robust threshold at each administrative control area, each area will be able to monitor quasi-static voltage instability at the entire interconnection level. Numerical simulations in the IEEE 300-bus system illustrate the effectiveness of the proposed performance index and the threshold.**

***Index Terms*—Distributed monitoring, overlapping decomposition, voltage stability, wide-area monitoring and control.**

I. Introduction

THIS paper is motivated by the need for a systematic framework that improves situational awareness in large-scale power system operations. With an increasing penetration of spatially dispersed and temporally variable resources into power grids, operators in power systems now face a much broader set of operating conditions than the traditional norms. Failure to recognize the changes in system-wide operating conditions may have led to the August 2003 Blackout, and may well lead to other similar events. This creates the fundamental need to utilize near real-time data obtained from massively deployed sensors such as phasor measurement units (PMUs) for wide-area monitoring, protection, and control (WAMPAC) in interconnected power systems [1], [2].

In particular, the objective of this paper is to introduce and test a *distributed* framework for monitoring potential quasi-static voltage collapse in interconnected multi-area power systems. Theoretically, quasi-static voltage instability is detected by the near singularity of the centralized power flow Jacobian matrix [3]–[5] or related reduced order submatrices [6], or by the calculation of the rightmost eigenvalue or the smallest singular value (SSV) of the dynamic state Jacobian matrix [7]. Besides eigenvalue [8], [9] and SSV [10], [11], other performance indices, such as minimization of load voltage deviation [12], maximum loading point [13], and least damping ratio [14], are also widely used for voltage stability analysis. Reference [15] presents a new stability index based on the measurement of local voltage phasors. The index can identify the voltage collapse point when it is near zero. More recent papers also use the second order approximation of the saddle-node bifurcation surface [16] and the ant colony optimization [17] for instability detection.

In practice, online voltage stability monitoring is a critical function in modern control centers of interconnected power systems such as PJM, NYISO, and NEPOOL. The core of voltage stability analysis software in control areas utilizes a transfer limit calculator (TLC), which simulates the MW transfer capability based on the latest system snapshot obtained by the state estimator. The TLC determines collapse points corresponding to a set of pre-defined interfaces, which consist of a set of multiple high-voltage transmission lines. These interfaces are used to simulate typical scenarios of power transfer from generation surplus regions to load centers. The interfaces are selected based on the experiences of operators and lengthy off-ine studies. For example, in PJM, the APSOUTH interface is defined as a set of four 500-kV transmission lines that transfer power from PJM West to the load centers of PEPCO, BGE, and DOMINIAN. With the aid of the calculated transfer limits, the operators are able to monitor and control the MW flow on each interface continuously so as to minimize the risk of potential voltage collapse.

However, such a centralized scheme of voltage instability monitoring may not be effective under a much broader set of operating conditions for the following reasons: 1) The TLC needs a reliable state estimation solution as its starting point. It is often the case that the global state estimator may not converge reliably when the system is close to voltage collapse. 2) The pre-defined reactive interfaces may not be the real weakest transfer interfaces in the system due to the change of operating conditions, such as the transmission outages and the unstable output of renewable sources. 3) In order to obtain a reliable transfer limit, one requires an accurate equivalence of external systems, but this equivalence is either unavailable or results in a heavy computational burden.

Decentralized monitoring and control methods of voltage stability in interconnected power systems have been studied in the literature. Reference [18] creates a decentralized feedback linearizing control design using local measurements. It decouples the machine dynamics from the system dynamics and therefore

Manuscript received November 17, 2011; revised February 01, 2012; accepted March 07, 2012. Date of publication April 25, 2012; date of current version October 17, 2012. The work of the first two authors is supported in part by National Science Foundation EECS #1029873 and in part by Texas Engineering Experiment Station. Paper no. TPWRS-01118-2011.

L. Xie and Y. Chen are with the Department of Electrical and Computer Engineering, Texas A&M University, College Station, TX 77843 USA (e-mail: Lxie@ece.tamu.edu; hebe.cheny@neo.tamu.edu).

H. Liao is with Louis Dreyfus Highbridge Energy, Stamford, CT 06902 USA (e-mail: hwliao@ieee.org).

Color versions of one or more of the figures in this paper are available online at http://ieeexplore.ieee.org.

Digital Object Identifier 10.1109/TPWRS.2012.2191310

not every generator needs to be converted. References [19] and [20] put forward distributed algorithms for calculating optimal power flow. Reference [21] employs local measurements of bus voltage and load current to measure the proximity to system voltage collapse, with the assumption that the rest of the system is treated as a Thevenin equivalence. Using this simple method, the system is completely distributed-only the measurements of each bus are needed to detect voltage problems. However, the nonlinearity of power systems renders the assumption of the Thevenin equivalence less accurate in a broad range of operating conditions.

In this paper, by exploring the structure of electric power networks, we propose a performance index which lends itself to distributed monitoring of system-wide quasi-static voltage collapse. This performance index is based on the sensitivity of the SSV of the decomposed power flow Jacobian matrix with respect to the regional loading levels. Overlapping decomposition is applied so that tie-line buses are included in both of the neighboring control areas. In this process most of the critical information of the centralized power flow Jacobian matrix is preserved [12], [22]. This performance index is 1) theoretically justifiable; 2) practically easy to implement as an indicator of potential voltage collapse; and 3) suitable for distributed monitoring in a WAMPAC framework.

The rest of this paper is organized as follows. The formulation and theoretical justification of the distributed performance index with overlapping decomposition is presented in Section II. A numerically robust threshold to indicate voltage collapse is also proposed. In Section III, the implementation of the distributed monitoring algorithm is presented. Section IV gives the numerical results for the IEEE 300-bus system and corresponding discussions. We draw conclusions and provide future research directions in Section V.

II. Proposed Performance Index for Distributed Voltage Collapse Monitoring

Large-scale power systems can be formulated by a coupled set of nonlinear differential and algebraic equations (DAEs) [23]

$$\dot{x} = f(x, u, y, p) \tag{1}$$

$$0 = g(x, u, y, p). \tag{2}$$

Define r as the number of generator buses, and s as the number of load buses. Assume we have constant load consumptions. Differential (1), where $f \in \mathbb{R}^{8r\times 1}$, contains the lectromechanical dynamics, electromagnetic dynamics, and excitation system dynamics of a generator. Algebraic (2), where $g \in \mathbb{R}^{(2r+2s)\times 1}$, represents the real and reactive power balance equations. $x \in \mathbb{R}^{8r\times 1}$ is the vector of generator internal state variables. $u \in \mathbb{R}^{2r\times 1}$ defines the generator control variables. $y \in \mathbb{R}^{2r\times 1}$ represents the algebraic variables—real and reactive power injections. p defines the system parameters.

Generally, the steady-state voltage stability of a power system is evaluated by monitoring the singularity of the system dynamic Jacobian matrix, which is the linearized version of DAEs (1) and (2), with algebraic (2) eliminated [5]. Elimination of (2) is based on the non-singularity of the power flow Jacobian matrix derived from (2)

$$J_0 = \begin{bmatrix} \frac{\partial P}{\partial \theta} & \frac{\partial P}{\partial V} \\ \frac{\partial Q}{\partial \theta} & \frac{\partial Q}{\partial V} \end{bmatrix} = \begin{bmatrix} J_{P\theta} & J_{PV} \\ J_{Q\theta} & J_{QV} \end{bmatrix} \tag{3}$$

where $J_0 \in \mathbb{R}^{(r+2s-1)\times(r+2s-1)}$; $P \in \mathbb{R}^{(r+s-1)\times 1}$ and $Q \in \mathbb{R}^{s\times 1}$ define the nodal injection of real and reactive power; $\theta \in \mathbb{R}^{(r+s-1)\times 1}$ and $V \in \mathbb{R}^{s\times 1}$ represent the phase angle and voltage magnitude of the buses. As the power system gets more and more stressed, the power flow Jacobian matrix J_0 will move closer to singularity. Therefore, the near singularity of matrix J_0 can be used as an effective tool for monitoring quasi-static voltage collapse [3], [10], [11].

Starting from our previous work in [22], we define a novel performance index (PI), which is based on the sensitivity of the SSV of the power flow Jacobian J_0 in (3) with respect to the regional loading levels. In contrast with commonly used PI, such as the SSV of the system-wide Jacobian, this new proposed PI allows effective distributed monitoring of system-wide voltage collapse. Based on the local measurements and state estimation, each control area can compute the PI and monitor the distance of system from voltage collapse. In what follows we provide the formulation and theoretical justification for the effectiveness of PI in distributed monitoring of quasi-static voltage collapse.

A. Centralized Performance Index

PI is defined as

$$PI = \left\| \frac{\partial\left(\frac{1}{\sigma_m}\right)}{\partial S} \right\|_\infty \tag{4}$$

where σ_m represents the SSV of the system-wide power flow Jacobian matrix J_0; $S = [S_1, S_2, \ldots, S_n]^T$ defines the apparent power of each bus with load; n is the total number of buses with load in the system.

Proposition 1: Consider the power system in DAEs (1) and (2). System-wide voltage collapse is about to happen when PI in (4) satisfies

$$PI^{Collapse} \geq \gamma \tag{5}$$

where γ is the threshold for monitoring voltage collapse, and will be given in the following section.

Proof: Assume each bus with load has a constant power factor, i.e.,

$$\frac{P_i}{Q_i} = a_i, \quad i = 1, 2, \ldots, n.$$

The apparent power injection at bus i could be represented as

$$S_i = \sqrt{P_i^2 + Q_i^2} = \sqrt{a_i^2 + 1} \cdot Q_i.$$

For bus i, the following expression holds:

$$\frac{\partial\left(\frac{1}{\sigma_m}\right)}{\partial Q_i} = \frac{-1}{\sigma_m^2} \cdot \frac{\partial \sigma_m}{\partial Q_i} = \frac{-1}{\sigma_m^2} \cdot \left(\frac{\partial V}{\partial Q_i}\right)^T \cdot \frac{\partial \sigma_m}{\partial V} \tag{6}$$

where $V = [V_1, V_2, \ldots, V_n]^T$ is the vector of voltage magnitude for buses with load.

A combination of (6) for all buses with load will result in

$$\underbrace{\frac{\partial\left(\frac{1}{\sigma_m}\right)}{\partial Q}}_{vector} = \underbrace{\frac{-1}{\sigma_m^2}}_{scalar} \cdot \underbrace{\left(J_{QV}^T\right)^{(-1)}}_{matrix} \cdot \underbrace{\frac{\partial \sigma_m}{\partial V}}_{vector} \tag{7}$$

where the superscript operator (-1) of the middle matrix defines the dot inverse of each element in the matrix. The last term $\partial\sigma_m/\partial V$ in (7) represents the sensitivity of the SSV of the power flow Jacobian matrix J_0 with respect to the voltage magnitude of each bus. Obtained from state estimation by the energy management system (EMS), the vector of voltage magnitude together with the phase angle can be used to construct the Jacobian matrix J_0. As a result, voltage magnitude will have an impact on the singularity of J_0, equivalently on σ_m. This indicates the implicit relationship of σ_m and V. What follows will be the nonzero property of $\partial\sigma_m/\partial V$. As the system gets more and more stressed, σ_m will move closer to zero, and $\left(J_{QV}^T\right)^{(-1)}$ will have larger elements. With the nonzero $\partial\sigma_m/\partial V$, $\partial\left(1/\sigma_m\right)/\partial Q$ in (7) will end up with larger and larger elements.

The proposed PI in (4) can be equivalently described as

$$PI = \max_i \left\{ \left| \frac{1}{\sqrt{a_i^2+1}} \cdot \frac{\partial\left(\frac{1}{\sigma_m}\right)}{\partial Q_i} \right| \right\}. \tag{8}$$

As σ_m moves closer to zero, PI will correspondingly become larger. When (5) is satisfied, $PI^{Collapse}$ will be detected, with σ_m equivalently having close to zero value. As a result, the potential system voltage collapse will be detected. □

Remark 1: As a commonly used PI, the SSV (σ_m) of the system-wide Jacobian has very small value near system singularity. This makes it difficult to monitor the proximity of σ_m to zero using the even smaller change of σ_m. Instead, the proposed PI in (4) holds a large value near system singularity, which makes it much easier for EMS to detect voltage collapse.

B. Overlapping Decomposition

The current existing interconnected power system is structured into different control areas that form the administrative boundaries. Each control area monitors and controls the power network within its boundary, and different control areas are interconnected via tie lines. For the power grid, each area can collect as much information as possible within its boundary. However, information exchange among areas is often limited due to the burden of communications. Under this condition, overlapping decomposition is employed to partition the whole system with tie-line-bus information included in both of the neighboring control areas. Since one can calculate the phase angle and voltage magnitude by power flow equations, using overlapping decomposition can help control areas achieve no information exchange, which will make relaxations for the communication burdens. The implementation of overlapping decomposition is described as follows.

A_k represents the set of buses inside control area k, and has the properties: $A_{k_1} \cap A_{k_2} = \varnothing$ for $k_1 \neq k_2$, and $\bigcup_{k=1}^{M} A_k = B$, where $B = \{B_1, B_2, \ldots, B_N\}$ is the set of buses, M is the total number of control areas, and N is the total number of system-wide buses.

T_k defines the set of tie-line buses directly connected to but outside control area k.

By overlapping decomposition, the system-wide power flow Jacobian matrix J_0 can be partitioned into an $M \times M$ block matrix. For any two neighboring control areas k and l connected via tie lines, the mathematical representation of overlapping decomposition can be described as

$$\begin{bmatrix} \Delta Y_{Ak} \\ \Delta Y_{Tkl} \\ \Delta Y_{Tlk} \\ \Delta Y_{Al} \end{bmatrix} = \begin{bmatrix} \frac{\partial Y_{Ak}}{\partial X_{Ak}} & \frac{\partial Y_{Ak}}{\partial X_{Tkl}} & 0 & 0 \\ \frac{\partial Y_{Tkl}}{\partial X_{Ak}} & \frac{\partial Y_{Tkl}}{\partial X_{Tkl}} & 0 & \frac{\partial Y_{Tkl}}{\partial X_{Al}} \\ \frac{\partial Y_{Tlk}}{\partial X_{Ak}} & 0 & \frac{\partial Y_{Tlk}}{\partial X_{Tlk}} & \frac{\partial Y_{Tlk}}{\partial X_{Al}} \\ 0 & 0 & \frac{\partial Y_{Al}}{\partial X_{Tlk}} & \frac{\partial Y_{Al}}{\partial X_{Al}} \end{bmatrix} \begin{bmatrix} \Delta X_{Ak} \\ \Delta X_{Tkl} \\ \Delta X_{Tlk} \\ \Delta X_{Al} \end{bmatrix} \tag{9}$$

where $k, l = 1, 2, \ldots, M$, $k \neq l$. The first two rows represent control area k. Y_{Ak} stands for P_k and Q_k in set A_k, while Y_{Tkl} represents P_k and Q_k in set T_k; X_{Ak} refers to θ_k and V_k in set A_k, and X_{Tkl} defines θ_k and V_k in set T_k. The last two rows represent control area l with similar notations holding.

For control area k, if the nonzero off-diagonal blocks in (9) are neglected, the lost information is about the buses in area l that are directly connected to the tie-line buses. These buses are defined as the "Second Level Bus (SLB)" for area k with the tie-line bus defined as the "First Level Bus (FLB)." Due to the structure of electric power networks, the high sparsity holds for the off-diagonal blocks, which also have smaller elements than do the diagonal blocks. Therefore the impact of neglecting the SLB in area k will be small.

With the acceptable neglect of the off-diagonal blocks in (9), the decentralized power flow Jacobian matrix for control area k could be represented as

$$J_k = \begin{bmatrix} \frac{\partial Y_{Ak}}{\partial X_{Ak}} & \frac{\partial Y_{Ak}}{\partial X_{Tk}} \\ \frac{\partial Y_{Tk}}{\partial X_{Ak}} & \frac{\partial Y_{Tk}}{\partial X_{Tk}} \end{bmatrix} = \begin{bmatrix} J_{AAk} & J_{ATk} \\ J_{TAk} & J_{TTk} \end{bmatrix} \tag{10}$$

which has a lower dimension and therefore the advantage of saving computational time and complexity for area k. For realistic large-scale interconnected power systems, this computational advantage enables the proposed method for real-time operations. Furthermore, taking the tie-line-bus information into consideration, overlapping decomposition preserves most of the critical information of the system-wide power flow Jacobian matrix and will perform more accurately.

C. Distributed Performance Index

From Proposition 1, the near singularity of the system-wide power flow Jacobian matrix J_0 results in system-wide $PI^{Collapse}$ satisfying (5). This PI can be used as an effective indicator for monitoring potential voltage problems. In

this section, we will use a similar definition as (4) to define a decentralized PI_d that can be employed to monitor system-wide voltage collapse by control areas in a distributed manner.

Define decentralized PI_d of control area k as

$$PI_{dk} = \left\| \frac{\partial \left(\frac{1}{\sigma_{mdk}} \right)}{\partial S_{dk}} \right\|_{\infty} \tag{11}$$

where σ_{mdk} is the SSV of the decentralized power flow Jacobian matrix J_k in (10); S_{dk} is the vector of apparent power for the buses with load in area k. The decentralized PI_d has a similar definition to system-wide PI in (4), except that σ_{md} and S_d are the regional variables.

Proposition 2: Consider the power system in DAEs (1) and (2). System-wide voltage collapse is about to happen when there exists at least one control area k whose PI_{dk} satisfies

$$PI_{dk}^{Collapse} \geq \gamma \tag{12}$$

where γ is the threshold for monitoring voltage collapse.

Proof: Assume the system-wide power flow Jacobian matrix J_0 is partitioned as (3). When J_0 is nonsingular, block diagonal dominance of J_0 will hold [24]. By using the Gerschgorin Circle Theorem [25] and its generalization [26]–[28], the SSV of J_0 will lie in the union of two disks. The center of each disk is the SSV of diagonal block $J_{P\theta}$ or J_{QV}. The corresponding radius of each disk is the largest singular value (LSV) of off-diagonal block J_{PV} or $J_{Q\theta}$.

Similarly, for area k, the decentralized Jacobian J_k in (10) can also be represented in the form of

$$J_k = \begin{bmatrix} J_{P\theta k} & J_{PVk} \\ J_{Q\theta k} & J_{QVk} \end{bmatrix}.$$

For each control area, σ_{md} will lie in the union of two disks, with the SSV of the diagonal blocks being the centers and the LSV of the off-diagonal blocks being the radius.

Define

$$\sigma_{mm} = \min \{\sigma_{mdk}\} \tag{13}$$

as the smallest one among the SSV of all control areas. σ_{mm} can be treated as the reconstructed SSV using all decentralized J_k.

Recall the reason J_k could be described in (10) is that the off-diagonal blocks of (9) are highly sparse with small elements. Mathematically this reason could be represented as

$$\left\| \begin{bmatrix} 0 & 0 \\ 0 & \frac{\partial Y_{Tkl}}{\partial X_{Al}} \end{bmatrix} \right\|_{\infty} \leq \beta_1, \left\| \begin{bmatrix} \frac{\partial Y_{Tlk}}{\partial X_{Ak}} & 0 \\ 0 & 0 \end{bmatrix} \right\|_{\infty} \leq \beta_2$$

that is, the largest elements of the off-diagonal blocks could be bounded by some real numbers β_1 and β_2. Because of the physically stronger interconnections of the buses in sets A_k and T_k than those in the SLB, β_1 and β_2 will always be smaller than the infinite norm of the diagonal blocks in (9). This can further demonstrate the feasibility of neglecting the SLB. Under this condition, the union of the eigenstructure of each area will reconstruct that of the original system. As a result, when the system is near singularity, σ_{mm} will satisfy

$$\left| \frac{\sigma_{mm} - \sigma_m}{\sigma_m} \right| \leq \epsilon. \tag{14}$$

The bounded error ϵ is set to be 0.1, which means σ_{mm} is sufficiently close to the system-wide σ_m.

Based on the above analysis, assume area k contributes σ_{mm} in (13). The corresponding PI_{dk} will satisfy

$$PI_{dk} = \max_i \left\{ \left| \frac{1}{\sqrt{a_i^2 + 1}} \cdot \frac{\partial \left(\frac{1}{\sigma_{mm}} \right)}{\partial Q_{dki}} \right| \right\} \tag{15}$$

where

$$\frac{\partial \left(\frac{1}{\sigma_{mm}} \right)}{\partial Q_{dki}} = \frac{-1}{\sigma_{mm}^2} \cdot \frac{\partial \sigma_{mm}}{\partial Q_{dki}} = \frac{-1}{\sigma_{mm}^2} \cdot \left(\frac{\partial V_{dk}}{\partial Q_{dki}} \right)^T \cdot \frac{\partial \sigma_{mm}}{\partial V_{dk}}. \tag{16}$$

σ_{mm} getting closer to zero will result in PI_{dk} becoming larger. When (12) is satisfied, $PI_{dk}^{Collapse}$ will be detected and the corresponding σ_{mm} will hold a close to zero value. With the relationship of (14), the system-wide σ_m is also close to zero, which can indicate that $PI^{Collapse}$ satisfies (5). In other words, $PI_{dk}^{Collapse}$ can indicate system collapse. As long as there exists one area k that has $PI_{dk}^{Collapse}$ satisfying (12), system-wide voltage collapse could be detected. □

D. Threshold for Distributed Monitoring

Proposition 2 provides a distributed way to monitor system-wide voltage collapse. To detect $PI_{dk}^{Collapse}$, a robust way to define the threshold is in great need.

Because of the definition of PI_{dk} in (11) and the differences in system characterizations, PI_{dk} will be system sensitive. Under this condition, each control area should first take regional system and load characterizations into consideration, and then define a normal value, PI_{dk}^{Normal}, as the regional base value for PI_{dk}. This normal value determination should be conducted before online monitoring. Corresponding procedures are described as follows.

Prior to real-time implementation, each control area collects the historical load data and conducts offline learning to find an appropriate reference, PI_{dk}^{Normal}. In order to find PI_{dk}^{Normal}, control areas should concentrate on the load with relatively lower values, typically around trough values of daily load. This could increase the contrast between the stressed PI_{dk} detected around the peak values of daily load and the reference, and therefore give an early alert for voltage collapse. Within typical seasonal cycles, time interval in which load data are around trough values can to be determined by statistical analysis. After that, offline calculation of PI_{dk} in that interval can be conducted using (11). Then, PI_{dk}^{Normal} is defined as the mean value of all the PI_{dk} in that interval. Because of the differences in system and load characterizations, the time interval will be different, and also PI_{dk}^{Normal} will vary for different control areas.

After the offline calculation of PI_{dk}^{Normal}, control areas obtain the precondition for online monitoring. In order to employ

a robust threshold, control area k needs to compare PI_{dk} from online calculation with PI_{dk}^{Normal}, that is, to compute the ratio

$$\tau_k(j) = \frac{PI_{dk}(j)}{PI_{dk}^{Normal}} \tag{17}$$

where $PI_{dk}(j)$ is PI_{dk} at the jth time step. $\tau_k(j)$ equivalently represents the relative change of $PI_{dk}(j)$ for the jth step. Therefore, the change of PI_{dk} for each step is of interest to the system operator, rather than the actual value of PI_{dk}.

Under normal conditions, area k will not have a very high load, which means the load will stay in the time interval determined for PI_{dk}^{Normal} for most of the time. This will result in the value of τ_k staying around 1. Due to the normalized definition of τ_k in (17), it is reasonable to specify $\tau_k^{Normal} \approx 1$, which is robust for all control areas. Therefore, it is easier for EMS of control area k to monitor τ_k for voltage problem detection. The following proposition is to sum up the above statement.

Proposition 3: Consider the power system in DAEs (1) and (2). System-wide voltage collapse is about to happen when there exists at least one control area k whose τ_k satisfies

$$\tau_k \geq \bar{\gamma} \tag{18}$$

where $\bar{\gamma} = 10$ is a robust threshold for all control areas.

Remark 2: We could set $\bar{\gamma} = 10$ since 10 times larger than τ_k^{Normal} could be treated as significantly large based on engineering experience and simulation practice, where $\tau_k(j)$ represents the relative change of $PI_{dk}(j)$ for the jth time step as compared with that of normal loading conditions. A change of 10 times of PI would indicate the closeness to ill condition of the system.

III. Implementation of Distributed Monitoring Algorithm

Based on the discussions in the previous section, the proposed PI is specifically tailored for the distributed monitoring of system-wide quasi-static voltage collapse. In this section, we present the algorithm for distributed online monitoring of quasi-static voltage collapse in multi-area power systems.

The implementation flowchart for control area k, where $k = 1, 2, \ldots, M$, is presented in Fig. 1. Steps 1 to 7 are conducted by EMS of area k. EMS of the system operator will implement Step 8. Online monitoring is conducted from Steps 2 to 8.

Step 1) Offline Learning: Determine PI_{dk}^{Normal} by offline study using historical data.
Step 2) Perform state estimation.
Step 3) Construct Jacobian matrix $J_k(j)$ by (10).
Step 4) Compute SSV (j) of $J_k(j)$.
Step 5) Calculate $PI_{dk}(j)$ by (11).
Step 6) Find normalized ratio $\tau_k(j)$ by (17).
Step 7) Once $\tau_k(j)$ satisfies (18), go to **Step 8**. Otherwise, return to **Step 2**.
Step 8) System operator receives alert from area k and EMS conducts system-wide corrective control.

In the next section, the IEEE 300-bus system will be employed to illustrate the effectiveness of the proposed PI and the threshold for distributed monitoring of quasi-static voltage collapse.

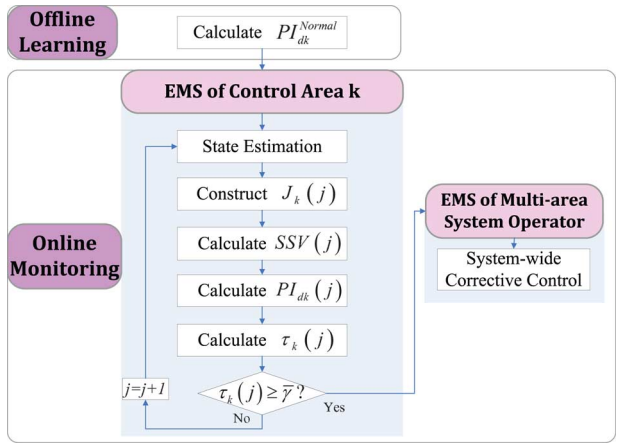

Fig. 1. Implementation of distributed monitoring algorithm for area k.

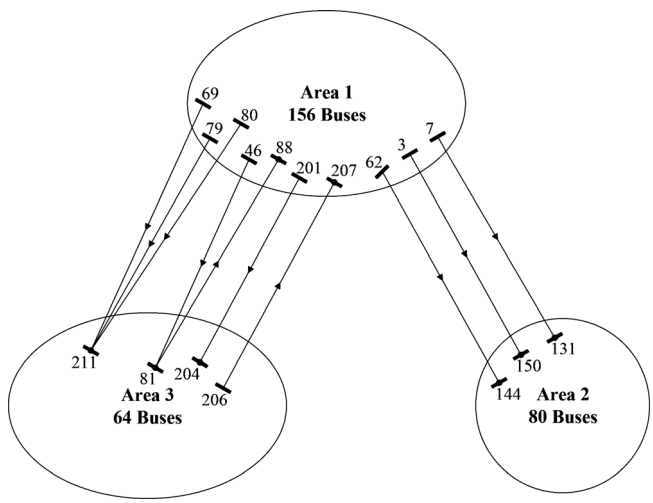

Fig. 2. System sketch for the IEEE 300-bus system with 3 control areas.

IV. Numerical Illustration

To demonstrate the effectiveness of the distributed PI_d and the threshold, the IEEE 300-bus system is employed in simulation. The simulation is conducted in $MatPower$ [29]. It is assumed that voltage collapse happens if the power flow equations fail to converge in 100 iterations with a tolerance of 10^{-6}.

The whole system is decomposed into three control areas. The Electric Reliability Council of Texas (ERCOT) load data for July 29, 2011 is used. The load data of weather zones "East," "North," and "West" are scaled to show the trends of load change for the three control areas. In order to simulate instability, the load levels are extended by interpolation. The change rate of load for the buses within one area is specified as the same. Local generators are employed to balance the incremental real power until the power flow equations fail to converge.

A graphic illustration of the IEEE 300-bus system is presented in Fig. 2. Tie lines are shown with bus numbers and the directions of power flow.

Figs. 3–6 employ 4-subplot figures with cyan plus, pink pentagram, blue square and black circle curves to present the simulation results of the centralized system and control areas 1, 2, and 3, respectively. The horizontal axis represents real time

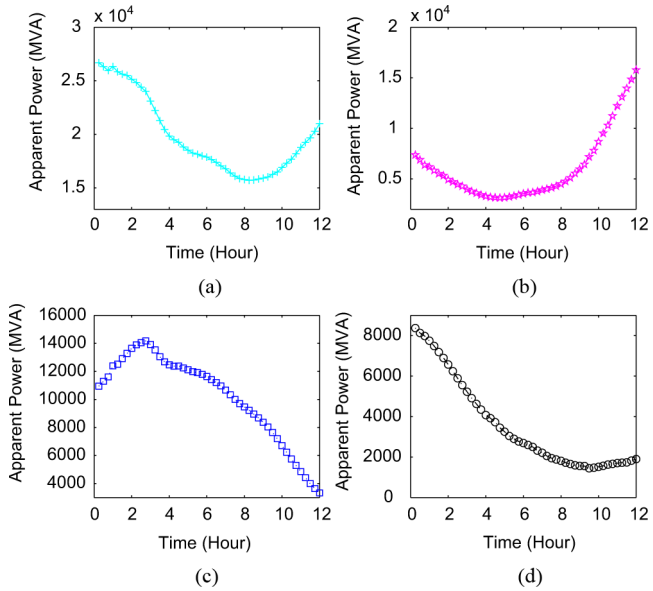

Fig. 3. Actual load for IEEE 300-bus system. (a) System-wide load. (b) Load in Area 1. (c) Load in Area 2. (d) Load in Area 3.

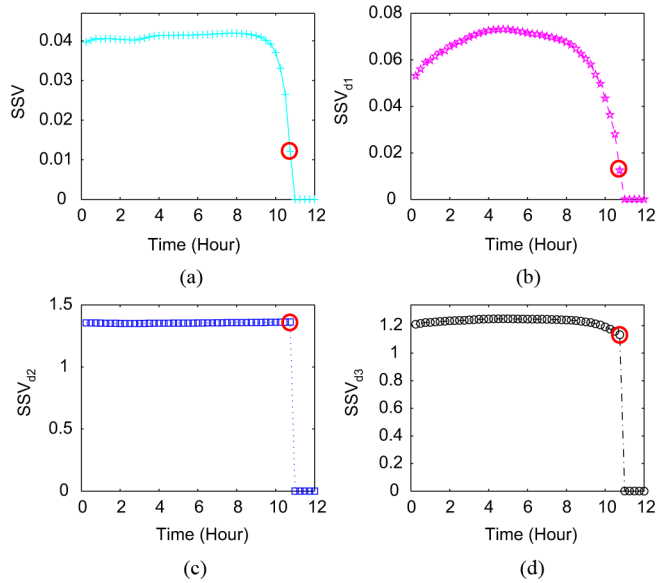

Fig. 4. SSV for IEEE 300-bus system. (a) SSV of system-wide Jacobian J_0. (b) SSV of Area 1 Jacobian J_1. (c) SSV of Area 2 Jacobian J_2. (d) SSV of Area 3 Jacobian J_3.

with a time interval of 15 min between 2 points. The subplot in (a) showing the overall system condition is employed to illustrate the effectiveness of the distributed monitoring method. The power flow equations stop converging at the 44th iteration, which represents 11:00 am, so all the figures are shown from 12:00 am to about 12:00 pm. Potential voltage collapse needs to be detected before 11:00 am to leave enough time for the system operator to perform corrective control.

Using scaled load data from ERCOT, the load is depicted in Fig. 3. For areas 2 and 3 the loads are shifted to get distinguished from that of area 1.

The SSV of the system-wide Jacobian matrix J_0 and the decentralized Jacobian matrix J_k are depicted in Fig. 4. It can be seen that the SSV change slightly with different values during the early time periods. Near the voltage collapse point at 11:00 am, the SSV for all subplots have large and fast drops. The points enclosed by red circles are defined as the $(n-1)$ point, $\mathrm{SSV}_{(n-1)}$, representing one iteration step before voltage collapse. These points are calculated at 10:45 am. The centralized SSV (σ_m) can indicate the proximity of a quasi-static limit using subplot (a) in Fig. 4. However, as stated in Remark 1, the change of σ_m is so small that a simple record of σ_m cannot provide a clear indication of system voltage collapse. Table I presents an illustration of this. It shows the values of the centralized and decentralized SSV at some typical iterations. The last column of Table I represents the numerical value of ϵ in (14). At the 43rd iteration, σ_{md1} is very close to σ_m, with the error of 3.01%. In other words, σ_{md1} is the σ_{mm} defined in (13). This can demonstrate the statement of Proposition 2 and also make σ_{md1} satisfy (14).

PI for the centralized system and the control areas are presented in Fig. 5, with Fig. 6 showing the zoomed-in figure. During the early time period, the changes in PI are relatively small, which is due to the slight changes in corresponding SSV and loading levels. In Fig. 6, the points enclosed by red circles are the $(n-1)$ point at 10:45 am, denoted by $PI_{(n-1)}$. It is

TABLE I
COMPARISON OF EIGENSTRUCTURE OF CENTRALIZED AND DECENTRALIZED JACOBIAN

Iteration	SSV_{cen}	SSV_1	SSV_2	SSV_3	Min(Error)
1	0.0397	0.0531	1.3354	1.2093	33.84%
24	0.0415	0.0715	1.3540	1.2466	72.20%
40	0.0370	0.0434	1.3603	1.1901	17.09%
41	0.0331	0.0363	1.3607	1.1749	9.75%
42	0.0265	0.0280	1.3611	1.1582	5.60%
43	**0.0121**	**0.0125**	1.3615	1.1335	**3.01%**

worthwhile to explain the fluctuations of area 3 in subplot (d) of Fig. 6. The fluctuation starts around 9 am. From the definition in (11), the value of PI_{dk} mainly depends on the change of $1/\sigma_{mdk}$ with respect to the change of regional loading level. As shown in Figs. 3 and 4, during the fluctuation interval, the numerator $1/\sigma_{mdk}$ decreases slightly and almost uniformly, while the regional load has some small fluctuations, resulting in too small changes between two steps. With almost the same numerator, the smaller denominator will lead to a larger PI_{d3}. However, what will be seen following is that given the choice of the threshold (PI being 10 times larger than that in normal conditions), these fluctuations are small enough as not to create any false alarms of voltage collapse. It is observed that the proposed method is robust enough against load fluctuations within normal conditions.

Table II presents the values of centralized PI and decentralized PI_d at some typical iterations. As long as PI_d is sufficiently large to satisfy (12) or (18), $PI_d^{Collapse}$ can be used to detect system-wide voltage collapse. Therefore it is of no need to compute ϵ for PI. As the system approaches voltage collapse, centralized PI and decentralized PI_{d1} both increase quickly. That is because σ_m and σ_{m1} are both small, and the terms $1/\sigma^2$ in (7) and (16) make the changes of PI and PI_{d1} even faster. This demonstrates the advantage of PI stated in Remark 1.

Although PI indicates system voltage problems well, the values of PI_d vary for different areas as can be seen from

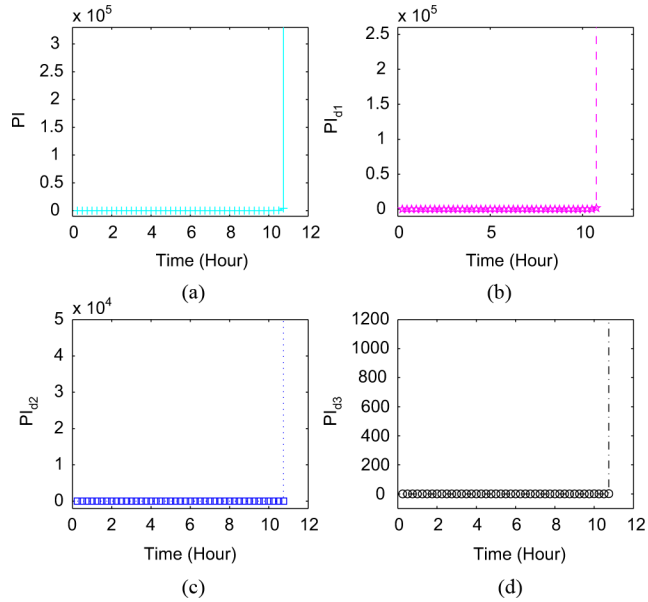

Fig. 5. PI for IEEE 300-bus system. (a) System-wide PI. (b) $\mathrm{PI_{d1}}$ for Area 1. (c) $\mathrm{PI_{d2}}$ for Area 2. (d) $\mathrm{PI_{d3}}$ for Area 3.

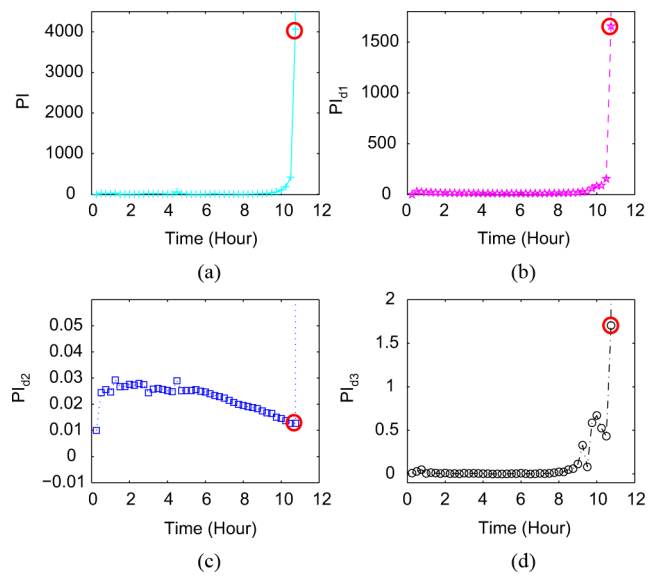

Fig. 6. Zoomed-in PI for IEEE 300-bus system. (a) Zoomed-in system-wide PI. (b) Zoomed-in $\mathrm{PI_{d1}}$ for Area 1. (c) Zoomed-in $\mathrm{PI_{d2}}$ for Area 2. (d) Zoomed-in $\mathrm{PI_{d3}}$ for Area 3.

TABLE II
COMPARISON OF CENTRALIZED PI AND DECENTRALIZED PI_d

Iteration	PI_{cen}	PI_{d1}	PI_{d2}	PI_{d3}
2	24.04	30.35	0.0245	0.0299
24	4.43	11.05	0.0247	0.0088
40	104.72	83.92	0.0146	0.6710
41	185.52	89.17	0.0137	0.5253
42	420.64	155.8	0.0127	0.4337
43	**4.07E3**	**1.66E3**	0.0127	1.7036

Table II. Therefore, the determination of PI_{dk}^{Normal} and the calculation of ratio τ are necessary to perform a robust threshold. For this kind of hot summer day, the normal value of load exists at the beginning of the day, as shown in subplot

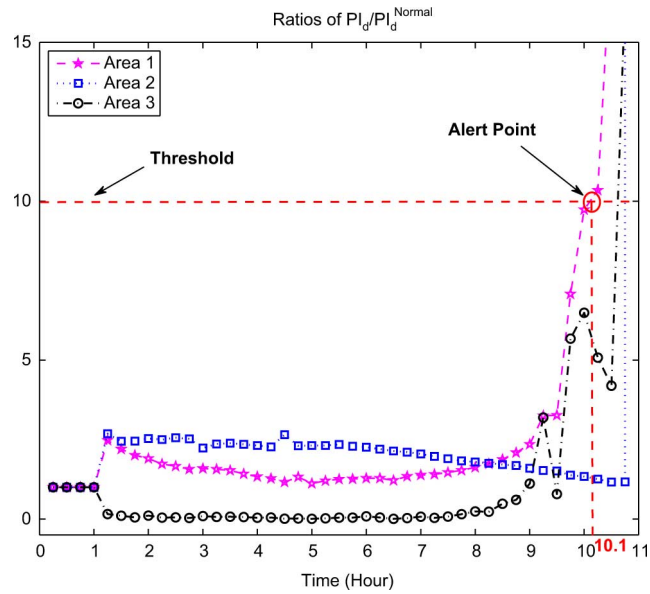

Fig. 7. Distributed monitoring for IEEE 300-bus system.

(b) of Fig. 3 without time shifting. So the load data from 5:00 am to 9:00 am for area 1 are specified as the base load and are used to calculate corresponding PI_{d1}^{Normal}. Similar procedures are performed for areas 2 and 3 with certain time shifting. The normal values for each area are $PI_{d1}^{Normal} = 8.6219$, $PI_{d2}^{Normal} = 0.0109$, and $PI_{d3}^{Normal} = 0.1034$. During online monitoring, each area takes new load data for each iteration and follows the algorithm in Section III.

Fig. 7 depicts the ratio τ for each control area, and Fig. 8 shows the zoomed-in performance. During the early time period with base regional loading levels, the ratios τ have some relatively small values around 1. The existence of small fluctuations due to those of PI_{dk} will not cause any false alarms. More offline learning will be needed to get a more accurate normal value of PI_{dk}^{Normal} and reduce the risk of false alarms. Moreover, with $\bar{\gamma} = 10$, the alert point reported from area 1 is at about 10:10 am in Fig. 8. This is even 35 min earlier than the $(n-1)$ point at 10:45 am. From these two figures, the system operator could also tell that area 1 is more prone to voltage collapse. So after receiving the alert from area 1, the system operator will have more than 35 min to perform system-wide corrective control. The value of $\bar{\gamma}$ could be adjusted to some lower level to provide the system operator more time for corrective control. In this way, a potential voltage collapse could be detected even earlier as can be seen from Fig. 7.

It is worthwhile to discuss the advantages of the overlapping decomposition used in this paper. From (9) to (10), the information of the SLB is neglected. The simulation results shown in Table I illustrate that the error of SSV is very small (3.01%), which further demonstrates the small error of using overlapping decomposition. A comparison of the proposed overlapping decomposition (OD_1) is given with the revised overlapping decomposition (OD_2), which takes the SLB into account. Table III presents the values of the SSV and PI at the $(n-1)$ point for comparison. In the first two rows, the results show that the SSV of OD_2 has a much larger error than that of OD_1.

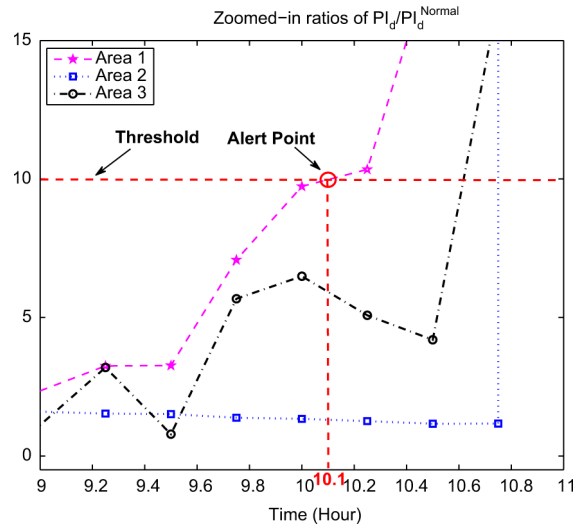

Fig. 8. Zoomed-in distributed monitoring for IEEE 300-bus system.

TABLE III
COMPARISON OF OVERLAPPING DECOMPOSITION

	System	Area 1	Area 2	Area 3	Min(Error)
SSV(OD_1)	0.0121	0.0125	1.3615	1.1335	3.01%
SSV(OD_2)	0.0346	0.0428	1.3986	1.2026	23.70%
$PI(OD_1)$	4.07E3	1.66E3	0.0127	1.7036	NA
$PI(OD_2)$	314.05	261.84	0.5724	0.0468	NA

This counterintuitive result is due to the existence of larger external impacts from the neighboring areas on voltage stability. In the last two rows, the results show that the PI of OD_2 gives almost as good an indication of voltage problems as that of OD_1, since both have large values satisfying (12) near system singularity. However, the larger error of SSV by OD_2 indicates a violation of (14) and makes the resulting PI_d less accurate. This is one shortcoming of OD_2. Furthermore, to get information about the SLB, area-level information exchange is needed, and therefore package loss and communication delay may occur. This makes it more difficult to perform OD_2. Another advantage of overlapping decomposition is the reduction of computational burden. The average computational time for calculating the centralized and decentralized SSVs is $t_{cen} = 0.18s$, $t_1 = 0.04s$, $t_2 = 0.007s$, and $t_3 = 0.005s$. This indicates that even for this 300-bus test, distributed method saves significantly computational time compared with the centralized method. When implemented in large-scale realistic power systems, the proposed method is expected to have significant computational time saving compared with the centralized approach. To sum up, the proposed overlapping decomposition not only is effective for distributed monitoring of voltage problems, but also can be easily implemented in reality and reduce computational burden. Since the information about tie-line buses could be obtained by power flow analysis, the proposed overlapping decomposition will help the control areas achieve the goal of no area-level information exchange and realize the real-time operations.

V. CONCLUSION

This paper presents a novel performance index for online monitoring of system-wide quasi-static voltage instability in a distributed way. The performance index is based on the sensitivity of the SSV of the distributed power flow Jacobian matrix with respect to the regional loading levels. Overlapping decomposition is employed to decompose the system into different control areas based on administrative rules. Theoretical justification is presented for the effectiveness of decentralized PI_d, and a normalized ratio is put forward for the control areas to obtain a robust threshold for monitoring system-wide voltage collapse. Each control area can calculate its PI_d and ratio τ in a lower dimension using the information of the regional buses and the tie-line buses without area-level information exchange.

The IEEE 300-bus system is employed in simulation to illustrate the effectiveness of the proposed performance index and the threshold. The results of the simulation demonstrate that the proposed performance index could indicate system-wide quasi-static voltage collapse in a distributed manner. With the defined performance index, the difference between system performances under stressed and normal conditions is enlarged, which makes it easier for EMS to detect voltage collapse. With the definition of ratio τ, the threshold $\bar{\gamma}$ presents the robustness for different control areas to monitor in a distributed way. By monitoring the occurrence of alerts in different areas, the system operator will be able to determine which area is more prone to future voltage collapse incidents. By choosing the appropriate threshold, the proposed monitoring method provides enough lead time to allow the system operator to perform corrective control before the ultimate voltage collapse. From the simulation, the objective to monitor system-wide quasi-static voltage collapse in a distributed way with minimum information exchange among administrative areas has been achieved.

From the effectiveness of our proposed method on the 300-bus system, it is reasonable to conjecture that our method is applicable to large-scale power systems. Further work will test the robustness and effectiveness of the proposed monitoring approach using realistic data. Practical implementation issues for the proposed monitoring framework, such as communication failure and computational parallelism, should also be future avenues of research. Future research will also focus on methodologies to increase stability margin and enhance voltage stability, using application of static VAR compensators (SVC) [30], or flexible AC transmission systems (FACTS) [31], and control aspects of dynamic voltage stability [32]. Last but not least, the proposed voltage collapse monitoring framework should be integrated as part of the future WAMPAC decision-making package for large-scale power systems.

REFERENCES

[1] V. Terzija, G. Valverde, D. Cai, P. Regulski, V. Madani, J. Fitch, S. Skok, M. M. Begovic, and A. Phadke, "Wide-area monitoring, protection, and control of future electric power networks," *Proc. IEEE*, vol. 99, no. 1, pp. 80–93, Jan. 2011.

[2] P. Kundur, J. Paserba, V. Ajjarapu, G. Andersson, A. Bose, C. Canizares, N. Hatziargyriou, D. Hill, A. Stankovic, C. Taylor, T. V. Cutsem, and V. Vittal, "Definition and classification of power system stability," *IEEE Trans. Power Syst.*, vol. 19, no. 2, pp. 1387–1401, May 2004.

[3] V. A. Venikov, V. A. Stroev, V. I. Idelchick, and V. I. Tarasov, "Estimation of electrical power system steady-state stability in load flow calculations," *IEEE Trans. Power App. Syst.*, vol. PAS-94, no. 3, pp. 1034–1041, May 1975.
[4] S. Grijalva and P. W. Sauer, "A necessary condition for power flow Jacobian singularity based on branch complex flows," *IEEE Trans. Circuits Syst. I*, vol. 52, no. 7, pp. 1406–1413, Jul. 2005.
[5] P. W. Sauer and M. A. Pai, "Power system steady-state stability and the load-flow Jacobian," *IEEE Trans. Power Syst.*, vol. 5, no. 4, pp. 1374–1383, Nov. 1990.
[6] X. Lei and D. Retzmann, "Static and dynamic approaches for analyzing voltage stability," *Eur. Trans. Elect. Power*, vol. 16, no. 3, pp. 277–296, May/Jun. 2006.
[7] H. Chiang, *Power System Stability*, ser. Wiley Encyclopedia of Electrical and Electronics Engineering, J. G. Webster, Ed. New York: Wiley, 1999, pp. 104–137.
[8] J. Rommes, N. Martins, and F. D. Freitas, "Computing rightmost eigenvalues for small-signal stability assessment of large-scale power systems," *IEEE Trans. Power Syst.*, vol. 25, no. 2, pp. 929–938, May 2010.
[9] Z. Du, C. Li, and Y. Cui, "Computing critical eigenvalues of power systems using inexact two-sided Jacobi-Davidson," *IEEE Trans. Power Syst.*, vol. 26, no. 4, pp. 2015–2022, Nov. 2011.
[10] P.-A. Löf, T. Smed, G. Andersson, and D. J. Hill, "Fast calculation of a voltage stability index," *IEEE Trans. Power Syst.*, vol. 7, no. 1, pp. 54–64, Feb. 1992.
[11] P.-A. Löf, G. Andersson, and D. J. Hill, "Voltage stability indices for stressed power systems," *IEEE Trans. Power Syst.*, vol. 8, no. 1, pp. 326–335, Feb. 1993.
[12] A. Zobian and M. D. Ilic, "A steady state monitoring and control algorithm using localized least square minimization of load voltage deviations," *IEEE Trans. Power Syst.*, vol. 11, no. 2, pp. 929–938, May 1996.
[13] L. A. L. Zarate and C. A. Castro, "A critical evaluation of a maximum loading point estimation method for voltage stability analysis," *Elect. Power Syst. Res.*, no. 70, pp. 195–202, 2004.
[14] A. Pama and G. Radman, "A new approach for estimating voltage collapse point based on quadratic approximation of PV-curves," *Elect. Power Syst. Res.*, no. 79, pp. 653–659, 2009.
[15] Y. Wang, W. Li, and J. Lu, "A new node voltage stability index based on local voltage phasors," *Elect. Power Syst. Res.*, no. 79, pp. 265–271, 2009.
[16] M. Perninge and L. Söder, "Risk estimation of the distance to voltage instability using a second order approximation of the saddle-node bifurcation surface," *Elect. Power Syst. Res.*, no. 81, pp. 625–635, 2011.
[17] C. Church, W. G. Morsi, M. E. El-Hawary, C. P. Diduch, and L. C. Chang, "Voltage collapse detection using ant colony optimization for smart grid applications," *Elect. Power Syst. Res.*, no. 81, pp. 1723–1730, 2011.
[18] J. W. Chapman, M. D. Ilic, C. A. King, L. Eng, and H. Kaufman, "Stabilizing a multimachine power system via decentralized feedback linearizing excitation control," *IEEE Trans. Power Syst.*, vol. 8, no. 3, pp. 830–839, Aug. 1993.
[19] G. Hug-Glanzmann and G. Andersson, "Decentralized optimal power flow control for overlapping areas in power systems," *IEEE Trans. Power Syst.*, vol. 24, no. 1, pp. 327–336, Feb. 2009.
[20] C. Lin and S. Lin, "Distributed optimal power flow with discrete control variables of large distributed power systems," *IEEE Trans. Power Syst.*, vol. 23, no. 3, pp. 1383–1392, Aug. 2008.
[21] K. Vu, M. M. Begovic, D. Novosel, and M. M. Saha, "Use of local measurements to estimate voltage-stability margin," *IEEE Trans. Power Syst.*, vol. 14, no. 3, pp. 1029–1035, Aug. 1999.
[22] L. Xie, J. Ilic, and M. D. Ilic, "Novel performance index and multi-layered information structure for monitoring quasi-static voltage problems," in *Proc. IEEE Power Engineering Society General Meeting, 2007*, Jun. 2007, pp. 1–7.
[23] M. D. Ilic, "From hierarchical to open access electric power systems," *Proc. IEEE*, vol. 95, no. 5, pp. 1060–1084, May 2007.
[24] A. Sode-Yome, N. Mithulananthan, and K. Y. Lee, "A maximum loading margin method for static voltage stability in power systems," *IEEE Trans. Power Syst.*, vol. 21, no. 2, pp. 799–808, May 2006.
[25] P. Lancaster and M. Tismenetsky, *The Theory of Matrices, Second Edition: With Application*. London, U.K.: Academic, 1985.
[26] C. Tretter, *Spectral Theory of Block Operator Matrices and Applications*. London, U.K.: Imperial College Press, 2008.
[27] M. D. Ilic, I. N. Katz, H. Dai, and J. Zaborszky, "Block diagonal dominance for systems of nonlinear equations with application to load flow calculations in power systems," *Math. Model.*, vol. 5, pp. 275–297, 1984.
[28] D. G. Feingold and R. S. Varga, "Block diagonally dominant matrices and generalizations of the Gerschgorin circle theorem," *Pacific J. Math.*, vol. 12, pp. 1241–1250, 1962.
[29] R. D. Zimmerman, C. E. Murillo-Sánchez, and R. J. Thomas, "MATPOWER steady-state operations, planning and analysis tools for power systems research and education," *IEEE Trans. Power Syst.*, vol. 26, no. 1, pp. 12–19, Feb. 2011.
[30] M. Z. El-Sadek, M. Dessouky, G. A. Mahmoud, and W. I. Rashed, "Series capacitors combined with static VAR compensators for enhancement of steady-state voltage stabilities," *Elect. Power Syst. Res.*, no. 44, pp. 137–143, 1998.
[31] A. R. Messina, M. A. Pérez, and E. Hernández, "Co-ordinated application of FACTS devices to enhance steady-state voltage stability," *Int. J. Elect. Power Energy Syst.*, no. 25, pp. 259–267, 2003.
[32] M. D. Ilic, E. H. Allen, J. W. Chapman, C. A. King, J. H. Lang, and E. Litvinov, "Preventing future blackouts by means of enhanced electric power systems control: from complexity to order," *Proc. IEEE*, vol. 93, no. 11, pp. 1920–1941, Nov. 2005.

Le Xie (S'05-M'10) received the B.E. degree in electrical engineering from Tsinghua University, Beijing, China, the M.Sc. degree in engineering sciences from Harvard University, Cambridge, MA, in 2005, and the Ph.D. degree in electrical and computer engineering from Carnegie Mellon University, Pittsburgh, PA, in 2009.

He is currently an Assistant Professor with the Department of Electrical and Computer Engineering, Texas A&M University, College Station. His industry experience includes an internship (June to August 2006) with ISO-New England and an internship with Edison Mission Energy Marketing and Trading (June to August 2007). His research interest includes modeling and control of large-scale complex systems, smart grid application with renewable energy resources, and electricity markets.

Yang Chen (S'12) received the B.E. degree in control science and engineering from Harbin Institute of Technology, Harbin, China, in 2010. She is pursuing the Ph.D. degree in the Department of Electrical and Computer Engineering at Texas A&M University, College Station.

Her research interests include voltage stability, power system analysis, modeling, and control of large-scale systems.

Huaiwei Liao (M'00) received the B.S. and M.S. degrees in electrical engineering from Chongqing University, Chongqing, China, and the Ph.D. degree in electrical and computer engineering from Carnegie Mellon University, Pittsburgh, PA, in 2011.

Currently, he is an Energy Trader and Director in the Department of Power Trading (FTR) at Louis Dreyfus Highbridge Energy, Stamford, CT. Before joining Louis Dreyfus in 2009, he was a Senior Energy Analyst with Edison Mission Group, Boston, MA, from 2008, MA; and a Power Engineer (Co-op) with the control center of PJM Interconnection, Norristown, PA, in 2006.